Received: May 16, 2022. Revised: July 4, 2022.

INASS

International Journal of
Intelligent Engineering & Systems

http://www.inass.org/

Resolving Interferometric SAR Speckle Problem Using Adaptive GAN

Hind Zeyada[1,2]* Sayed Abdo Mohamed[2] Gamal Tharwat[1]
Hany Harb[3] Ayman Nasr Hamed[2]

[1]*Faculty of Engineering, Al-Azhar University, Cairo, Egypt*
[2]*National Authority for Remote Sensing and Space Science (NARSS), Cairo, Egypt*
[3]*Information Technology College, Misr University for Science and Technology, Cairo, Egypt*
* Corresponding author's Email: sar.hend87@gmail.com

Abstract: The interference of reflected waves from multiple elementary scatterers produces speckle, which appears as a granular noise in synthetic aperture radar (SAR) images. These speckles in SAR images cause difficulty in image interpretation, which reduces the effectiveness of image segmentation and classification. In this paper, we propose an effective solution using generative adversarial networks (GAN) to decrease speckle noise while preserving texture features.The convolutional block attention module (CBAM) boosts the essential features in upsampled data and supports the creation of a final denoised real InSAR data.The proposed deep-learning method proved that CBAM enhanced the peak signal-to-noise ratio using the GAN. Furthermore, CBAM improved structural similarity (SSIM) to 99 and achieved the minimum mean squared error. The despeckle performance was enhanced using GAN-ResUNet in which the SSIM equals 0.999. The denoising performance proved that the use of GAN with CBAM as the generator inspired by ResUNeT achieved the best performance compared to other experiments results.

Keywords: InSAR, Speckle, GAN, CBAM.

1. Introduction

Synthetic aperture radar (SAR) collects images containing vital information about the surface of the Earth, as does any coherent imaging technique. However, speckle noise affects the processing accuracy. Recently, various speckle filtering algorithms have been proposed [1-4] and used in pre-processing to limit the impacts of speckle in these applications. Many such algorithms in the literature [5, 6] include Gaussian filtering, spatial-pixel feature denoising algorithm, and bilateral filtering used to handle various fundamental noise-removal tasks [7, 8]. Reducing speckle noise without losing some fine features of the SAR image is challenging. Thus, speckle makes SAR image processing and interpretation difficult.

Recently, deep learning (DL) has been advanced to performing several image-related tasks. The multilayer perceptron approach can effectively deal with image noise, but its use has been limited by the high training parameters [9]. The benchmarking tool [10] that depends on an accurate and well-tested SAR simulator, which can generate realistic SAR images while accounting for electromagnetic (EM) and geometric properties of the sensed surface, is used to overcome the availability of speckle-free images of Earth Observation (EO) missions.

Deep convolutional networks stack more convolutional layers to extract features and achieve clear images [10]. Generative adversarial network (GAN) [11] covered the way to significant progress on image generation and deblurring. GAN for image despeckling (ID-GAN) was proposed to automatically eliminate speckle from noisy input images [12]. The network was designed to minimize the perceptual difference between the restored and ground-truth images, as well as the Euclidean distance. Recently, attention modules have been useful in computer vision. The authors of [13] proved that GAN network can be improved more than their baseline networks, especially with target

objects. They observed quantitatively measured high performance in the interpretability of models.

In this paper used a DL strategy based on GANs to solve the interferometric InSAR image despeckling problem. Firstly, a deep residual U-Net based on generative advertisal network (GAN) was proposed. Secondly, proposed a deep U-Net and residual U-Net based GAN with embedded attention of CBAM. It improved the quality of the InSAR image by despeckling.

The InSAR images have a strong applications such as earthquakes, landslides, and volcanic eruptions, in addition, InSAR is the technology created in the 1970s to output topographic maps [14]. Finally, compared two proposed methods and the extensive experiments show that the network that embedded with CBAM has an effective results in despeckling the InSAR image. The residual U-Net as a motivation for the generator was used for the benefits of residual learning. Furthermore, The CBAM was applied [15] after the decoder component of the UNet to enhance relevant features. Technically, the ResUNet architecture addresses the gradient-vanishing problem and stabilizes the proposed GAN training. CBAM is an easily implementable module that progressively estimates channel and spatial attention; ithad demonstrated efficacy in object detection and classification tasks. The main contributions of this paper are concisely summarized as follows:

- We proposed a denoising GAN that uses adversarial training to automatically retrieve features from low-noise InSAR images and employed the CBAM attentionto reduce the speckles, resulting in clear images with accurate and realistic details.
- The generator inspired by ResUNet using CBAM attention of theGANwas applied to the InSAR data to suppress the noise while preserving structural information, making it suitable for this problem.
- The performance of the proposed GAN outperforms other approaches using simulated and real datasets.

The remainder of this paper is organized as follows: Section 2 reviews the related work on despeckling and the GAN. Section 3 presents the proposed methodology and architecture for InSAR despeckling approach. Section 4 discusses the design of the experiments, their results, and the outcomes. Finally, Section 5 presents the conclusion.

2. Related work

2.1 Denoising images based on conventional technique

The Boxcar filter is the most commonly used method. However, it performs poorly because it cannot distinguish between different targets. Lee et al. [16, 17] proposed speckle reduction techniques based on the multiplicative noise model and the minimum mean-square error (MMSE) criterion. Lee et al. [18] proposed the Refined Lee filter, a method for selecting neighbouring pixels with similar scattering characteristics. In a similar adaptive technique, other techniques use the local linear minimum mean squared error (LLMMSE) criterion proposed by Vasile et al. [19], but the decision to select homogeneous areas is based on the intensity information of the polarimetric coherency matrices, namely intensity-driven adaptive-neighborhood (IDAN).

2.2 Denoising images based on CNN

Several approaches have been presented to study the issue of InSAR data despeckling. In [20], the authors produced denoised targets by averaging multi-temporal images and detecting only regions unchanged during training. Other studies [21] used prior knowledge of the statistical model of noise to synthetically generate speckle images. DL approaches are widely used in remote sensing tasks owing to their capacity to automatically learn acceptable characteristics from images without explicitly defining the parameters of specific algorithms [22-26]. Recently, DL has been implemented for SAR despeckling jobs [27-29]. In [30], the authors proposed Image Despeckling Convolutional Neural Network (ID-CNN), a deep learning-based approach for automatically removing speckle from noisy input images. The proposed method outperforms state-of-the-art speckle reduction methods. Sparse-based machine learning methods, for example, have been used successfully in image denoising [31]. A non-locally centralised sparse representation (NCSR) method used nonlocal self-similarity to optimise the sparse method and achieve high performance for image denoising[32]. To reduce computational costs, a dictionary learning method was used to quickly filter the noise [33]. Prior knowledge (i.e., total variation regularisation) can smooth the noisy image to deal with the corrupted image and recover the detailed information of the latent clean image [34, 35]. [36-38] present more competitive image denoising

methods, such as the Markov random field (MRF) [39], weighted nuclear norm minimization (WNNM) [40], and learned simultaneous sparse coding (LSSC) [36]. Although the majority of the methods discussed above performed reasonably well in image denoising, they had several drawbacks, including the need for optimization methods during the testing phase, manual parameter setting, and a specific model for single denoising tasks. As architectures have become more flexible, deep learning techniques have recently gained the ability to overcome these drawbacks [41].

To improve the SAR image speckle problem, the deep encoder/decoder Convolutional Neural Network (CNN) architecture was presented, with a focus on specialized filtering capabilities and texture preservation [5]. The proposed DL-based despeckling approach (deSpeckNet) involves two stages: in the first stage, a supervised learning paradigm with a temporally averaged SAR image as a reference label is used, whereas in the second stage, unsupervised fine-tuning is employed to adjust a new noise distribution [42].

2.3 Denoising images based on GAN

Computer vision and DL-based image denoising techniques using a GAN containing a generator and a discriminator are presented in [43]. The generator creates a denoised image from a noisy input image, whereas the discriminator determines whether the image is real. A better loss function was used for the GAN's training. The generator weight changed during this adversarial training phase, resulting in a denoised image comparable to the ground-truth image. The main idea of the proposed method is to use representative features to implicitly regularize the discriminator. Residual learning approaches sometimes allow for greater performance by concentrating on forecasting the residual image, i.e., the noise, rather than immediately generating a denoised image [44].

In [45], DL using the GAN achieved high performance in many fields. Because the GAN consists of the generator and discriminator, the training of these two models provides realistic image outputs. In [46], the authors achieved the best measure performance using GAN in super-resolution GAN (SRGAN) and image restoration problem by recovering information in detail [47]. SRGAN can be used in different fields, such as medical images. In [48], a densely connected super-resolution network was used to recover information from brain magnetic resonance images in detail. In [49], a generator using U-Net was presented to restore images of magnetic resonance and enhance the definition. The target details of denoising problems, de-aliasing, and super-resolution were recovered as much as possible.

3. Methodology

The proposed architecture was build on the basis of residual learning, attention module and batch normalization to generate high-quality despeckled images. The GAN structure was We employed for image denoisingusing ResUNet. Next, Three residual blocks in our initial version was used due to timing constraints. Note, that more residual blocks may improve the measuring performance, but the training times may be extended.

3.1 Problem definition

Speckle is a naturally occurring problem in coherent imaging systems where the spatial resolution is greater than the wavelength. SAR is an example of such an imaging system. Due to the roughness of the surface, each resolution cell contains several scatterers. Thus, the resulting image has a granular appearance because of constructive and destructive interferences.The granularity of speckled images makes them difficult to interpret, both for the human eye and automated segmentation and classification algorithms, as presented in Fig. 1 [50].

A denoising problem can be expressed as a prediction process that converts HN images to LN images. Assume that the HN image is collected X and the ideal LN image is Y. Speckle noise Z is multiplicative noise, and this relationship can be expressed as in Eq. (1):

$$\mathrm{X} = Y.\mathrm{Z} \tag{1}$$

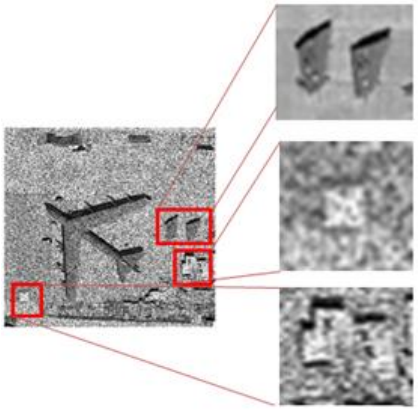

Figure. 1 Details of the patches of original and synthetic noise images

The goal of a statistical model is to estimate the noise distribution Z and obtain Y through an inverse operation. However, if we can obtain Y through a pre-processing method, DN-GAN can automatically extract the visual features of X and find an inverse mapping function f, which appears as $\hat{Y} = f.(\mathrm{X})$. As a result, prior knowledge, such as noise distribution, is superfluous. The image $\hat{Y}$ recovered by any algorithm cannot then be equal to Y,, and the gap R is as follows:

$$R = \hat{Y} - Y = u - v \tag{2}$$

where u denotes the residual speckle in $\hat{Y}$, and v is unrecovered detail. R is the gap, and Y is the clean image. The goal of GAN is to reduce the R gap. As a result, by subtracting u and adding v, a clean image Y can be obtained [51].

3.2 Proposed architecture

The implementation was present details of the proposed practical solution for the SAR despeckling method ResUNet-GAN, as shown in the network architecture in Fig. 2. It consists of two parts: a) adversarial learning framework for SAR image pair generation and its loss functions for optimization and b) the network architecture of the discriminator with modified ResUNet. This section formulates the despeckling SAR image problem using DL. In addition, we present a detailed description of the proposed ResUNet-GAN structure. The GAN network was designed to provide a score for both the generated and real images that can be seen as regression problem. If the network is efficiently trained, it will return a score close to 1 for the real label image, and 0 for the generated image, denoting that the network has robust ability to discriminate and can proficiently distinguish between true and fake images. In this study, after the image passing through the generator, the obtained image labels are clear images and the fake ones are noised images. The discriminator's network structure is simple that involves a series of convolutional layers which connect to the link layer before being sent to the tanh function to normalise the confidence score to a probability between 0 and 1.

3.2.1. Generator network

Single-image denoising is used to produce a high-quality image. The generator is used to the fact that the image noise is filled with surrounding pixels without losing any information from the original image.

The symmetric structure was employed a similar to that used in typical CNN frameworks to train an end-to-end mapping from noisy input images to their corresponding ground truth. In front of the network, three convolutional layers were stacked using batch normalization and ReLU activation to extract semantic information from the input image.

Furthermore, three residual blocks each with two convolutional layers were used to increase the network depth. Next, The symmetric was used to skip connections in this sub-network to boost training efficiency. The input was fed to the deep layers *via* skip connections that allow each residual layer to alter the output in proportion to the input while preserving the spatial information. The images were resized from 64 × 64 to 128 × 128, to 256 × 256 as the final image size.

Because the sub-pixel convolution is similar to deconvolution, we refer to those layers as deconvolutional layers. RELU activations were present in the first two deconvolutional layers, whereasSigmoid activations were used in the final deconvolutional layer, which gives the denoised output. All layers had a stride of one. The generator network model is based on U-Net as follows:

$$\begin{gathered} G = CBL(K) - CBL(K \otimes 2) - CBL(K \otimes 2 \otimes 2) \\ -CBL(K \otimes 2 \otimes 2) - CBL(K \otimes 2 \otimes 2) \\ -CBL(K \otimes 2 \otimes 2) - DBL(K \otimes 2) - DBL(k) \\ -DB(3) - Tanh \end{gathered} \tag{3}$$

where G is the generator, $CBL(K)$ is a set of K-channel convolutional layers followed by batch normalization and ReLU activation, and $DBL(k)$is a set of K-channel deconvolutional layers followed by batch normalization and ReLU activation.The generating network is such that for every two layers, skip connections are added [52].

3.2.2. Discriminator network

The purpose of speckle image denoising is to produce a solution that is visually pleasing and quantitatively comparable to the original and photo realistic. To categorize whether each input image is real or false, we inserted a learned discriminator sub-network. Throughout the discriminator network, The five convolutional networks was presented with batch normalization and ReLU activation [52].

$$\begin{gathered} D = CB(K2) - CBL(K2 \otimes 2) - CBL(K2 \otimes 2 \otimes 2) \\ - CBL(K2 \otimes 2 \otimes 2 \otimes 2) - C(1) \\ - Sigmoid \end{gathered} \tag{4}$$

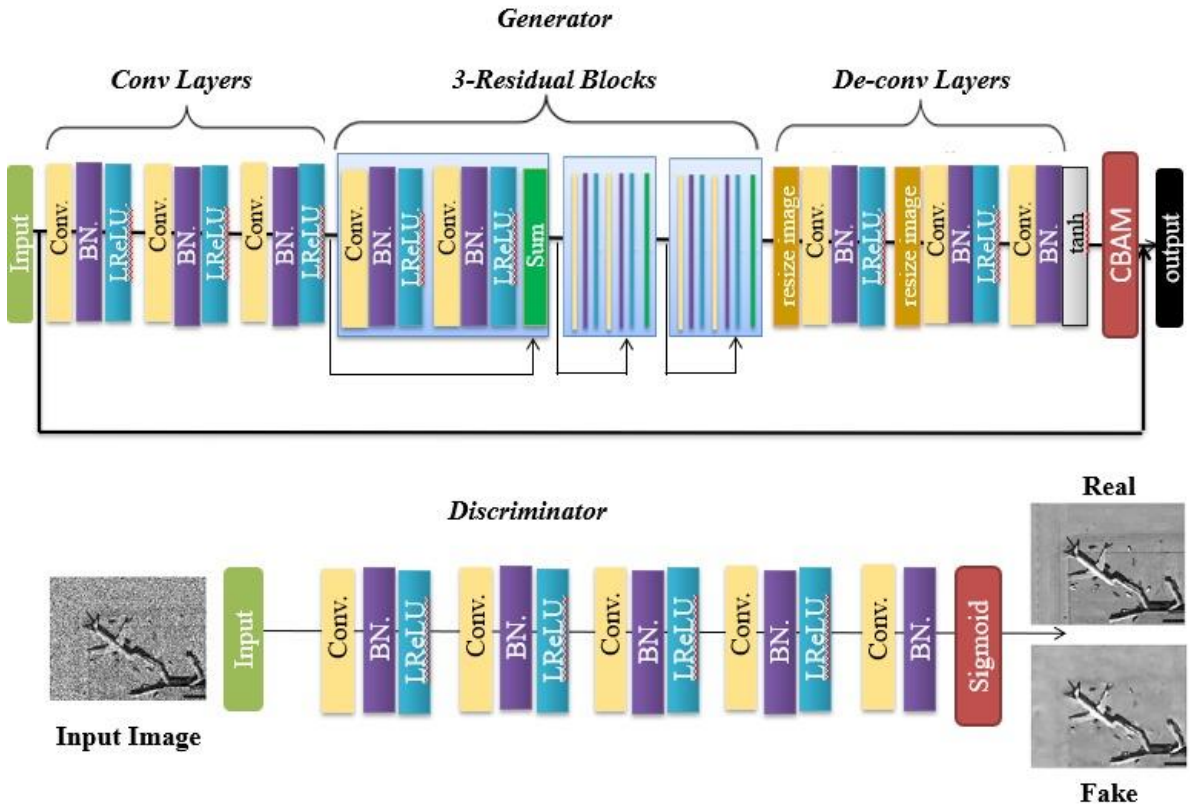

Figure. 2 Generator and discriminator layouts of the proposed GAN network structure

Where D is the discriminator, $CB(K2)$ denotes a collection of $K2$ channel convolutional layers followed by batch normalization, and $C(1)$ represents a set of one-channel convolutional layers.

3.2.3. Loss function

The pixel-to-pixel Euclidean loss (pixel loss) was combined, smooth loss, feature loss, and adversarial loss with appropriate weights to ensure that the results have good visual and quantitative scores as well as good discriminatory performance. Adversarial loss assists the generator in producing better output in order to deceive the discriminator. Feature loss aids in the accurate extraction of features and is calculated in the same manner as pixel loss, but is determined by examining image data extracted from the Conv2 layer of the VGG16 network. We supplement the existing loss functions with a smooth loss function. The reasoning behind this is to avoid "checkboard" artefacts across neighbouring pixels in the image. To calculate the smooth loss, we shift a copy of the generated image one unit to the left and one unit down, then compute the Euclidean distance between the shifted images. Following that, the new loss function is defined as follows:

$$L = \lambda_a L_a + \lambda_p L_p + \lambda_f L_f + \lambda_s L_s \quad (5)$$

where L_a denotes adversarial loss (discriminator loss), L_p denotes pixel loss (pixel-to-pixel Euclidian distance between generated image and ground truth image), L_f denotes feature loss (pixel-to-pixel Euclidian distance between generated image and ground truth image from the Conv2 layer of VGG16), and L_s denotes smooth loss. a, p, f and s are pre-defined weights for adversarial loss, pixel loss, feature loss, and smooth loss, respectively [52].

4. Experimental details and results

In this section, the details of our experiment investigating was discussd the proposed despeckle network and present which model enhances image quality and improves the performance measure.

4.1 Experimental setting

The proposed model was implemented using the PyTorch framework [53] and optimized by minimizing the loss function in Eq. (5) using the Adam algorithm. We trained the model using a minibatch size of 16 on an NVIDIA RTX 60002080 GPU with 24-GB onboard memory. The learning rate was initially set to 4E-7 for 1000 epochs.

Furthermore, The training data was pre-processed separately since a fully convolutional network was used for the generator. Its dimension is

256 × 256 pixels, which is useful for testing various ways because the redundant background and worthless regions are cropped out. However, the proposed architecture was evaluated using real InSAR images from the Sentinel-1A satellite. The proposed denoised images using the GAN architecture were statistically and qualitatively compared with traditional methods and validated. Experimental results indicated that the proposed ResU-Net-GAN architecture performs well even in HN environments and takes less computation time.

4.2 Evaluation metric

The comparison of the restored clean (denoised) images with ground-truth images serves as the basis for the evaluation. the mean squared error (MSE) was used conventional peak signal-to-noise ratio (PSNR), and structural similarity (SSIM) index [54], which is frequently used in the literature.

The MSE between two images, such as $X(n,m)$ and $\hat{Y}(n,m)$, is defined as follows[55]:

$$MSE = \frac{1}{MN}\sum_{n=0}^{M}\sum_{m=1}^{N}[\hat{Y}(n,m) - X(n,m)]^2 \quad (6)$$

PSNR is expressed as:

$$PSNR = 10\ log_{10}(pealval^2)/MSE \quad (7)$$

where peakval (Peak Value) is maximal in the image data. If it is an 8-bit unsigned integer data type, the peakval is 255 [56].

$$SSIM_{(x,y)} = \left[l_{(x,y)}\right]^{\propto}.\left[c_{(x,y)}\right]^{\beta}.\left[s_{(x,y)}\right]^{\gamma} \quad (8)$$

where l is the luminance (used to compare the brightness between two images), c is the contrast (used to compare the ranges between the brightest and darkest regions of two images), s is the structure (used to compare the local luminance pattern between two images to find the similarity and dissimilarity of the images), and $\propto, \beta$, and γ are the positive constants [57].

4.3 Datasets

Virtual SAR dataset: It is a synthetic dataset collected from NWPU-RESISC45 that includes 5500 images. Each pair is of size 256 ×256 pixels. It was used to enhance the performance of the denoising task.

Real dataset: The Sentinel-1A Single Look Complex (SLC) real dataset containing 1350 images with a size of 256 ×256 pixels was used in the experiments. They were acquired in the interferometric wide swath mode using the terrain observation with progressive scan (TOPS) technique [58]. Furthermore, they were acquired in C-band for both single and dual polarizations. The GRD images were multilooked to five looks in the range direction and projected to ground range using an Earth ellipsoid model by the data provider.

The dataset was randomly split to 60%, 20%, and 20% for training, validation, and testing, respectively. Note, the data augmentation was never used during training.

4.4 Analysis and results

The analysis of the quantitative measures, namely, PSNR, SSIM, and MSE using different GANs, is presented in Table 1. The generator and discriminator of the GAN model were concurrently trained. Based on this, the time for running the GAN model was longer than that for traditional methods. The best performance was evaluated using the minimum parameters of the GAN model.

The proposed methods are based on DL GAN-UNet and GAN-ResUNet with CBAM attention; The numerous experiments was conducted on the synthetic InSAR and Sentinel-1A datasets. Then, the denoised images was compared with reference images and evaluated the results. The comparison between these methods was performedby calculating the degree of similarity between the denoised and reference images. The proposed deep network proved that CBAM enhanced the PSNR using the GAN and its generator inspired by ResUNet by 5.87 dB through a comparison of the 3^{rd} and 4^{th} rows of Table 1. Also, CBAM improved SSIM from 0.92 to 0.95.

The result presented in Table 1 demonstrates that the use of synthetic noise in the training set improves data diversity and model robustness. The despeckle performance was enhanced for the proposed GAN-ResUNet with CBAM in which PSNR equals 21.42 compared with other experimental results of convolutional neural network method and GAN based noise method in [30] and [59] respectively.

Although, the SSIM metric of the methods in [30] and [59] are better than the proposed one. The Visual interpretation of the images of the proposed method is easier. In addition they have more clear features as shown in Fig. 3. The obtained images of the methods in [30] and [59] are more smooth which the image features are lost as shown in Fig. 3.

Table 2 shows the performance comparison of the proposed GAN using Sentinel-1A images. The results indicate that using a training set containing

Table 1. Performance comparison between the proposed GAN and other basline approaches using synthetic InSAR images

Methods	MSE	SSIM	PSNR
CNN Method [30]	0.018	0.97	21.09
GAN Method [59]	0.0204	0.998	17.94
GAN-Unet+CBAM	0.0194	0.998	18.3
GAN-ResUNet	0.0198	0.999	18.17
GAN-ResUNet+CBAM	0.0187	0.999	18.42

Table 2. Performance comparison between the proposed GAN and other basline approaches using real InSAR images

Methods	MSE	SSIM	PSNR
CNN Method [30]	0.011	0.98	20.65
GAN Method [59]	0.0126	0.96	19.86
GAN-Unet+CBAM	0.014	0.96	19.58
GAN-ResUNet	0.0319	0.924	15.55
GAN-ResUNet+ CBAM	0.0089	0.95	21.42

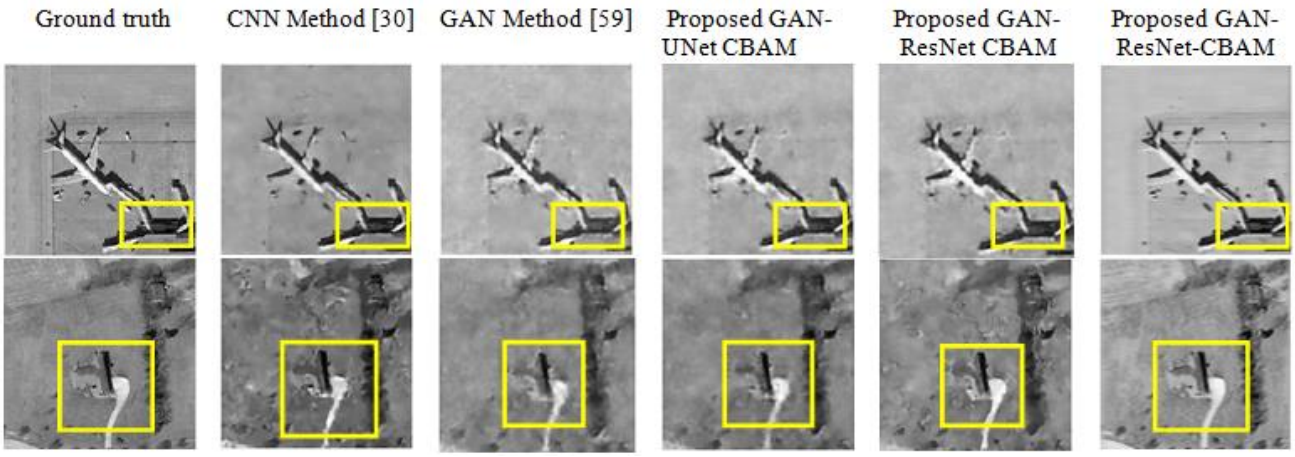

Figure. 3 Comparison between Virtual SAR dataset denoising methods

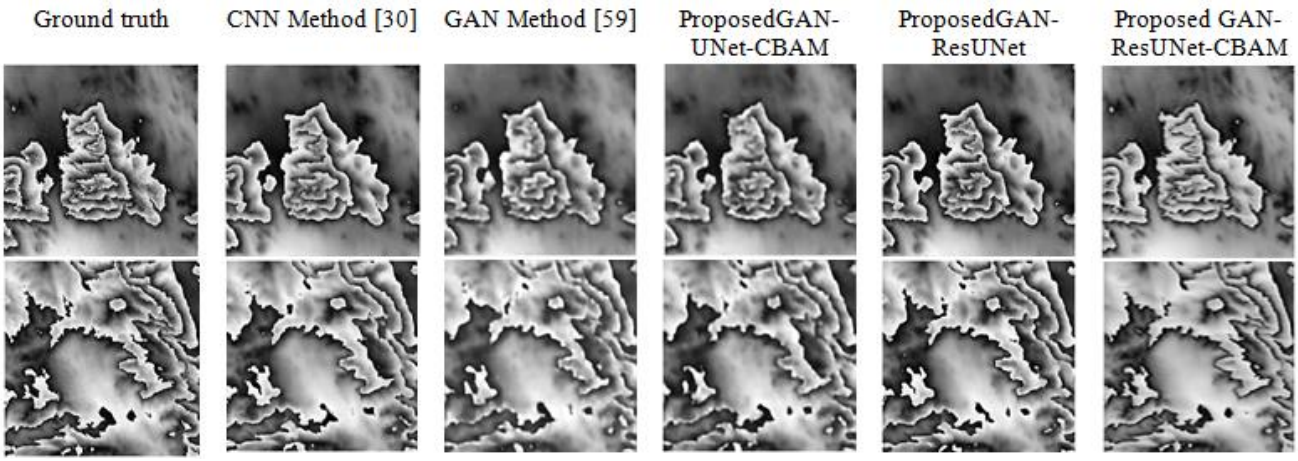

Figure. 4 Comparison between real dataset denoising methods

real noise increases the diversity of the InSAR data and the robustness of the model. The denoising performance was enhanced for GAN-ResUNet using CBAM attention, which improved SSIM compared with the other experiments of methods used in [30], [59]. The generator inspired by ResUNet has achieved the best SSIM and increased the performance to be 0.999. The improvement increased in proposed network of a deep residual U-Net based on generative advertisal (GAN) by 0.029 using SSIM. The images quality of the proposed methodare appeared more clear than images quality using models in [30] and [59], in addition to the easy visual interpretation features as shown in Fig. 4.

The despeckled results from different models are achieved to solve the interferometry of InSAR noise images. The generator was used inspired by UNet and ResUNet and applied with the GAN. The CBAM module was added after the UNet and ResUNet decoder components to improve the speckle filter and retain the quality of the features.

The ideal place for CBAM in this model is used after the decoder component in both experiments. Thus, that CBAM was conclude boosted essential features in upsampled data and supported the

creation of a final denoised image for the following convolution layer. The effectiveness of CBAM was found to rely on the network's complexity, as presented in Fig. 3 and 4.The despeckled results from different GAN models of the interferometric SAR data are presented in Fig.3. The 6th column representing the GAN model whose generator is inspired by ResUNET and the CBAM attention shows the details of the fringe features more than the other models. The real images of the used InSAR data are wrapped images. Thus, the generator model of the 6th column is essential in the despeckling process.

Compared with other techniques, GAN proved to have high performance in despeckling and detail. preservation while shortening the test time, thereby making it more practical for applications.

5. Conclusion

In this paper, an improved network architecture was proposed for InSAR image denoising. The experiments of GAN network was compared using two generators inspired by the UNet and Res-UNet models using CBAM attention. These models automatically remove speckle noise and improve the quality of the InSAR data. Synthetic data were used to increase the training data, and the encoding block was added to the generator to improve the usable features for despeckling. Compared with alternative methods for speckle reduction in InSAR data. The proposed method has significant advantages: 1) GAN obtained the best despeckling performance with fewer parameters than other basline approaches models, and the generated images were more real. 2) Compared with other approaches, the proposed model exhibits high performance in despeckling and detail retention with the quickest operating time, making it perfect for many applications. The denoising performance was improved using the GAN with CBAM attention as the generator inspired by UNet and ResUNet.

Conflicts of Interest

The authors declare no conflict of interest.

Author Contributions

Conceptualization, Hind Zeyada. and Sayed Abdo; methodology, Sayed Abdo, Gamal Tharwat, and Hany Harb; software, Hind Zeyada and Gamal Tharwat ;validation, Ayman Nasr and Hany Harb; formal analysis, Hind Zeyada; Sayed Abdo and Gamal Tharwat writing—original draft preparation, Hind Zeyada and Sayed Abdo; writing— review and editing, Hind Zeyada; Sayed Abdo and Ayman Nasr; visualization, Hany Harb and Ayman Nasr.

References

[1] Z. Xu, S. Sun, C. Yang, and X. Zhang, "A Comparative Study on the Current De-speckle Methods for Polarimetric Synthetic Aperture Radar Imagery Processing", In: *Proc. of MIPPR 2015: Remote Sensing Image Processing, Geographic Information Systems, and Other Applications*, p. 98150R, 2015.

[2] S. W. Chen, X. C. Cui, X. S. Wang, and S. P. Xiao, "Speckle-free SAR Image Ship Detection", *IEEE Transactions on Image Processing*, Vol. 30, pp. 5969-5983, 2021.

[3] K. Dasari and L. Anjaneyulu, "Importance of Speckle Filter Window Size and its Impact on Speckle Reduction in SAR Images", *International Journal of Advances in Microwave Technology*, Vol. 2, No. 2, pp. 98-102, 2017.

[4] A. Shanthasheela and P. Shanmugavadivu, "An Exploratory Analysis of Speckle Noise Removal Methods for Satellite Images", In: *Proc. of the 2018 International Conference on Electronics and Electrical Engineering Technology*, pp. 217-222, 2018.

[5] F. Lattari, B. G. Leon, F. Asaro, A. Rucci, C. Prati, and M. Matteucci, "Deep Learning for SAR Image Despeckling", *Remote Sensing*, Vol. 11, No. 13, p. 1532, 2019.

[6] V. Santhi, D. Mohandass, J. Jayanthi, P. Arulmozhivarman, and R. Mehra, "Speckle Reduction in SAR Images Using CNN", In: *Proc. of 2021 3rd International Conference on Signal Processing and Communication*, pp. 223-227, 2021.

[7] B. Goyal, A. Dogra, S. Agrawal, B. S. Sohi, and A. Sharma, "Image Denoising Review: From Classical to State-of-the-art Approaches", *Information Fusion*, Vol. 55, pp. 220-244, 2020.

[8] P. Singh, M. Diwakar, A. Shankar, R. Shree, and M. Kumar, "A Review on SAR Image and its Despeckling", *Archives of Computational Methods in Engineering*, Vol. 28, No, 7, pp. 4633-4653, 2021.

[9] L. Alzubaidi, J. Zhang, A. J. Humaidi, A. A. Dujaili, Y. Duan, O. A. Shamma, J. Santamaría, M. A. Fadhel, M. A. Amidie, and L. Farhan, "Review of Deep Learning: Concepts, CNN Architectures, Challenges, Applications, Future Directions", *Journal of Big Data*, Vol. 8, No. 1, pp. 1-74, 2021.

[10] G. D. Martino, A. D. Simone, A. Iodice, and D. Riccio, "Benchmarking Framework for Multitemporal SAR Despeckling", *IEEE Transactions on Geoscience and Remote Sensing*, Vol. 6, pp. 1-26, 2021.

[11] J. Y. Zhu, T. Park, P. Isola, and A. A. Efros, "Unpaired Image-to-image Translation Using Cycle-consistent Adversarial Networks", In: *Proc. of the IEEE International Conference on Computer Vision*, pp. 2223-2232, 2017.

[12] P. Wang, H. Zhang, and V. M. Patel, "Generative Adversarial Network-based Restoration of Speckled SAR Images", In: *Proc. of 2017 IEEE 7th International Workshop on Computational Advances in Multi-sensor Adaptive Processing*, pp. 1-5, 2017.

[13] R. R. Selvaraju, M. Cogswell, A. Das, R. Vedantam, D. Parikh, and D. Batra, "Grad-cam: Visual Explanations from Deep Networks via Gradient-based Localization", In: *Proc. of the IEEE International Conference on Computer Vision*, pp. 618-626, 2017.

[14] H. H. Zeyada, M. S. Mostafa, M. M. Ezz, A. H. Nasr, H. M. Harb, "Resolving Phase Unwrapping in Interferometric Synthetic Aperture Radar Using Deep Recurrent Residual U-Net", *The Egyptian Journal of Remote Sensing and Space Science*, Vol. 25, No. 1, pp. 1-10, 2022.

[15] S. Woo, J. Park, J. Y. Lee, and I. S. Kweon, "Cbam: Convolutional Block Attention Module", In: *Proc. of the European Conference on Computer Vision*, pp. 3-19, 2018.

[16] J. S. Lee, M. R. Grunes, and G. D. Grandi, "Polarimetric SAR Speckle Filtering and its Implication for Classification", *IEEE Transactions on Geoscience and Remote Sensing*, Vol. 37, No. 5, pp. 2363-2373, 1999.

[17] J. S. Lee, M. R. Grunes, and S. A. Mango, "Speckle Reduction in Multipolarization, Multifrequency SAR imagery", *IEEE Transactions on Geoscience and Remote Sensing*, Vol. 29, No. 4, pp. 535-544, 1991.

[18] J. S. Lee, M. R. Grunes, D. L. Schuler, E. Pottier, L. F. Famil, "Scattering-Model-Based Speckle Filtering of Polarimetric SAR Data", *IEEE Transactions on Geoscience and Remote Sensing*, Vol. 44, No. 1, pp. 176-187, 2005.

[19] G. Vasile, E. Trouvé, J. S. Lee, and V. Buzuloiu, "Intensity-Driven Adaptive-Neighborhood Technique for Polarimetric and Interferometric SAR Parameters Estimation", *IEEE Transactions on Geoscience and Remote Sensing*, Vol. 44, No. 6, pp. 1609-1621, 2006.

[20] G. Chierchia, D. Cozzolino, G. Poggi, and L. Verdoliva, "SAR Image Despeckling through Convolutional Neural Networks", In: *Proc. of 2017 IEEE International Geoscience and Remote Sensing Symposium*, pp. 5438-5441, 2017.

[21] J. Wang, T. Zheng, P. Lei, and X. Bai, "Ground Target Classification in Noisy SAR Images Using Convolutional Neural Networks", *IEEE Journal of Selected Topics in Applied Earth Observations and Remote Sensing*, Vol. 11, No. 11, pp. 4180-4192, 2018.

[22] L. Zhang, L. Zhang, and B. Du, "Deep Learning for Remote Sensing Data: A Technical Tutorial on the State of the Art", *IEEE Geoscience and Remote Sensing Magazine*, Vol. 4, No. 2, pp. 22-40, 2016.

[23] Y. Li, H. Zhang, X. Xue, Y. Jiang, and Q. Shen, "Deep Learning for Remote Sensing Image Classification: A Survey", *Wiley Interdisciplinary Reviews: Data Mining and Knowledge Discovery*, Vol. 8, No. 6, p. e1264, 2018.

[24] X. Wu, D. Hong, P. Ghamisi, W. Li, and R. Tao, "MsRi-CCF: Multi-scale and Rotation-insensitive Convolutional Channel Features for Geospatial Object Detection", *Remote Sensing*, Vol. 10, No. 12, p. 1990, 2018.

[25] Y. Zhen, H. Liu, J. Li, C. Hu, and J. S. Pan, "Remote Sensing Image Object Recognition based on Convolutional Neural Network", In: *Proc. of 2017 First International Conference on Electronics Instrumentation & Information Systems*, pp. 1-4, 2017.

[26] J. Tang, F. Zhang, F. Ma, F. Gao, Q. Yin, and Y. Zhou, "How SAR Image Denoise Affects the Performance of DCNN-Based Target Recognition Method", In: *Proc. of 2021 IEEE International Geoscience and Remote Sensing Symposium*, pp. 3609-3612, 2021.

[27] S. P. Cammarasana, P. Nicolardi, and G. Patanè, "A Universal Deep Learning Framework for Real-Time Denoising of Ultrasound Images", *arXiv Preprint arXiv:2101.09122*, 2021.

[28] A. B. Molini, D. Valsesia, G. Fracastoro, and E. Magli, "Speckle2Void: Deep Self-supervised SAR Despeckling with Blind-spot Convolutional Neural Networks", *IEEE Transactions on Geoscience and Remote Sensing*, Vol. 23, pp. 1-7, 2021.

[29] S. A. Mohamed, A. H. Nasr, and H. M. Keshk, "Three-Pass (DInSAR) Ground Change Detection in Sukari Gold Mine, Eastern Desert, Egypt", In: *Proc. of 2nd International*

Conference on Pervasive Computing and Social Networking, pp. 653-662, 2022.

[30] P. Wang, H. Zhang, and V. M. Patel, "SAR Image Despeckling using a Convolutional Neural Network", *IEEE Signal Processing Letters*, Vol. 24, No. 12, pp. 1763-1767, 2017.

[31] K. Dabov, A. Foi, V. Katkovnik, and K. Egiazarian, "Image Denoising by Sparse 3-D Transform-domain Collaborative Filtering", *IEEE Transactions on Image Processing*, Vol. 16, No. 8, pp. 2080-2095, 2007.

[32] W. Dong, L. Zhang, G. Shi, X. Li, "Nonlocally Centralized Sparse Representation for Image Restoration", *IEEE Transactions on Image Processing*, Vol. 22, No. 4, pp. 1620-1630, 2012.

[33] M. Elad and M. Aharon, "Image Denoising via Sparse and Redundant Representations over Learned Dictionaries", *IEEE Transactions on Image Processing*, Vol. 15, No. 12 pp. 3736-3745, 2006.

[34] S. Osher, M. Burger, D. Goldfarb, J. Xu, and W. Yin, "An Iterative Regularization Method for Total Variation-based Image Restoration", *Multiscale Modeling and Simulation*, Vol. 4, No. 2, pp. 460-489, 2005.

[35] D. Ren, W. Zuo, D. Zhang, L. Zhang, and M. H. Yang, "Simultaneous Fidelity and Regularization Learning for Image Restoration", *IEEE Transactions on Pattern Analysis and Machine Intelligence*, Vol. 43, No. 1, pp. 284-299, 2019.

[36] J. Mairal, F. Bach, J. Ponce, G. Sapiro, A. "Zisserman, Non-local Sparse Models for Image Restoration", In: *Proc. of 2009 IEEE 12th International Conference on Computer Vision*, pp. 2272-2279, 2009.

[37] W. Zuo, L. Zhang, C. Song, D. Zhang, and H. Gao, "Gradient Histogram Estimation and Preservation for Texture Enhanced Image Denoising", *IEEE Transactions on Image Processing*, Vol. 23, No. 6, pp. 2459-2472, 2014.

[38] K. Zhang, W. Zuo, Y. Chen, D. Meng, L. Zhang, "Beyond Agaussian Denoiser: Residual learning of deep cnn for Image Denoising", *IEEE Transactions on Image Processing*, Vol. 26, No. 7, pp. 3142-3155, 2017.

[39] U. Schmidt and S. Roth, "Shrinkage Fields for Effective Image Restoration", In: *Proc. of the IEEE Conference on Computer Vision and Pattern Recognition*, 2014.

[40] S. Gu, L. Zhang, W. Zuo, and X. Feng, "Weighted Nuclear Norm minimization with Application to Image Denoising", In: *Proc. of the IEEE Conference on Computer Vision and Pattern Recognition*, pp. 2862-2869. 2014.

[41] A. Lucas, M. Iliadis, R. Molina, and A. K. Katsaggelos, "Using Deep Neural Networks for Inverse Problems in Imaging: Beyond Analytical Methods", *IEEE Signal Processing Magazine*, Vol. 35, No. 1, pp. 20-36, 2018.

[42] A. G. Mullissa, D. Marcos, D. Tuia, M. Herold, and J. Reiche, "despecknet: Generalizing Deep Learning-based SAR Image Despeckling", *IEEE Transactions on Geoscience and Remote Sensing*, Vol. 17, pp. 1-5, 2020.

[43] M. J. Hasan, M. S. Alom, U. Fatema, and M. F. Wahid, "Deep Learning Based Retinal OCT Image Denoising Using Generative Adversarial Network", In: *Proc. of 2021 International Conference on Automation, Control and Mechatronics for Industry 4.0*, pp. 1-6, 2021.

[44] Y. Guo, Q. Jin, G. Facciolo, T. Zeng, and J. M. Morel, "Residual Learning for Effective Joint Demosaicing-Denoising", *arXiv Preprint arXiv:2009.06205*, 2020.

[45] I. Goodfellow, J. P. Abadie, M. Mirza, and B. Xu, D. W. Farley, S. Ozair, A. Courville, and Y. Bengio, "Generative Adversarial Nets", *Advances in Neural Information Processing Systems*, Vol. 27, 2014.

[46] C. Ledig, L. Theis, F. Huszár, J. Caballero, A. Cunningham, A. Acosta, A. Aitken, A. Tejani, J. Totz, Z. Wang, and W. Shi, "Photo-realistic Single Image Super-resolution Using a Generative Adversarial Network", In: *Proc. of the IEEE Conference on Computer Vision and Pattern Recognition*, pp. 4681-4690, 2017.

[47] M. S. Moustafa and S. A. Sayed, "Satellite Imagery Super-Resolution Using Squeeze-and-Excitation-Based GAN", *International Journal of Aeronautical and Space Sciences*, Vol. 22, No. 6, pp. 1481-1492, 2021.

[48] Y. Chen, F. Shi, A. G. Christodoulou, Y. Xie, Z. Zhou, and D. Li, "Efficient and Accurate MRI Super-resolution Using a Generative Adversarial Network and 3D Multi-level Densely Connected Network", In: *Proc. of International Conference on Medical Image Computing and Computer-Assisted Intervention*, pp. 91-99, 2018.

[49] G. Yang, S. Yu, H. Dong, G. Slabaugh, P. L. Dragotti, X. Ye, F. Liu, S. Arridge, J. Keegan, Y. Guo, and D. Firmin, "DAGAN: Deep De-aliasing Generative Adversarial Networks for Fast Compressed Sensing MRI Reconstruction", *IEEE Transactions on Medical Imaging*, Vol. 37, No. 6, pp. 1310-1321, 2017.

[50] A. Foi, V. Katkovnik, and K. Egiazarian, "Pointwise Shape-adaptive DCT for High-quality Denoising and Deblocking of Grayscale and Color Images", *IEEE Transactions on Image Processing*, Vol. 16, No. 5, pp. 1395-1411, 2007.

[51] Z. Chen, Z. Zeng, H. Shen, X. Zheng, P. Dai, and P. Ouyang, "DN-GAN: Denoising generative Adversarial Networks for Speckle Noise Reduction in Optical Coherence Tomography Images", *Biomedical Signal Processing and Control*, Vol. 55, p. 101632, 2020.

[52] A. Alsaiari, R. Rustagi, M. M. Thomas, and A. G. Forbes, "Image Denoising Using a Generative Adversarial Network", In: *Proc. of 2019 IEEE 2nd International Conference on Information and Computer Technologies*, pp. 126-132, 2019.

[53] F. Chollet, *Keras Documentation*, keras. io, 2015.

[54] Z. Wang, A. C. Bovik, H. R. Sheikh, and E. P. Simoncelli, "Image Quality Assessment: From Error Visibility to Structural Similarity", *IEEE Transactions on Image Processing*, Vol. 13, No. 4, pp. 600-612, 2004.

[55] J. Søgaard, L. Krasula, M. Shahid, D. Temel, K. Brunnström, and M. Razaak, "Applicability of Existing Objective Metrics of Perceptual Quality for Adaptive Video Streaming", *Electronic Imaging*, Vol. 2016, No. 13, pp. 1-7, 2016.

[56] R. G. Deshpande, L. L. Ragha, and S. K. Sharma, "Video Quality Assessment through PSNR Estimation for Different Compression Standards", *Indonesian Journal of Electrical Engineering and Computer Science*, Vol. 11, No. 3, pp. 918-924, 2018.

[57] R. Kumar and V. Moyal, "Visual Image Quality Assessment Technique Using FSIM", *International Journal of Computer Applications Technology and Research*, Vol. 2, No. 3, pp. 250-254, 2013.

[58] R. Scheiber, M. Jäger, P. P. Iraola, F. D. Zan, and D. Geudtner, "Speckle Tracking and Interferometric Processing of TerraSAR-X TOPS Data for Mapping Nonstationary Scenarios", *IEEE Journal of Selected Topics in Applied Earth Observations and Remote Sensing*, Vol. 8, No. 4, pp. 1709-1720, 2014.

[59] L. D. Tran, S. M. Nguyen, and M. Arai. "GAN-based Noise Model for Denoising Real Images.", In: *Proc. of the Asian Conference on Computer Vision*, 2020.